



HAL
open science

Slowness and azimuth determination for Bucovina array (BURAR) applying multiple signal techniques

Felix Borleanu, Mihaela Popa, Mircea Radulian, Johannes Schweitzer

► To cite this version:

Felix Borleanu, Mihaela Popa, Mircea Radulian, Johannes Schweitzer. Slowness and azimuth determination for Bucovina array (BURAR) applying multiple signal techniques. *Journal of Seismology*, 2011, 15 (3), pp.431-442. 10.1007/s10950-011-9228-9 . hal-00669209

HAL Id: hal-00669209

<https://hal.science/hal-00669209>

Submitted on 12 Feb 2012

HAL is a multi-disciplinary open access archive for the deposit and dissemination of scientific research documents, whether they are published or not. The documents may come from teaching and research institutions in France or abroad, or from public or private research centers.

L'archive ouverte pluridisciplinaire **HAL**, est destinée au dépôt et à la diffusion de documents scientifiques de niveau recherche, publiés ou non, émanant des établissements d'enseignement et de recherche français ou étrangers, des laboratoires publics ou privés.

Slowness and azimuth determination for Bucovina array (BURAR) applying multiple signal techniques

Felix Borleanu · Mihaela Popa ·
Mircea Radulian · Johannes Schweitzer

Received: 20 July 2009 / Accepted: 13 January 2011
© Springer Science+Business Media B.V. 2011

Abstract The BURAR seismic array, located in Northern Romania (Bucovina region), is designed to monitor events located in an area poorly covered by other existing seismic stations. In order to use the BURAR array for single-station locations, it is crucial to calibrate the azimuth and slowness parameters, which are currently used in array techniques to locate earthquakes, blasts or nuclear explosions. The goal of this study is to apply “f–k” and plane wave fit techniques in order to constrain the slowness and azimuth parameters at BURAR for teleseismic, regional and local events. The analysis was carried out using P and S waves recorded for events occurred between 2004 and 2008 within a radius of 50° around BURAR. The azimuth values obtained applying both methods strongly deviated from the theoretical values for regions like Central Turkey, Bulgaria, Dodecanese Islands and part of Greece, while the ray parameter deviations with respect to a 1-D IASP91 reference model are less significant. For the local events, the anomalies are smaller, except

the particular case of Vrancea intermediate-depth earthquakes for which strong azimuth deviations (33.5°), both positive and negative, are observed. We investigate how these systematic deviations in azimuth are explained by the structure lateral heterogeneities which characterize the study region.

Keywords Array techniques · f–k analysis · Plane wave fit · BURAR array

1 Introduction

Seismological arrays can be used in many different ways to study the lateral heterogeneities from the lithosphere and upper mantle structure. For this purpose, many different, specialized array techniques have been developed and applied to an increasing number of high-quality array datasets. Most of these methods use the ability of seismic arrays to measure the velocity of an incident wave front and its backazimuth. This information can be used to distinguish between different seismic phases, separate waves from different seismic events and improve the signal-to-noise ratio (SNR) by stacking with respect to the varying slowness of different phases (e.g., Schweitzer et al. 2002).

The Bucovina array (BURAR) is located in the northern part of Romania in the neighborhood

F. Borleanu (✉) · M. Popa · M. Radulian
National Institute for Earth Physics,
Magurele, Romania
e-mail: felix@infp.ro

J. Schweitzer
NORSAR, Instituttveien 25 2007 Kjeller, Norway

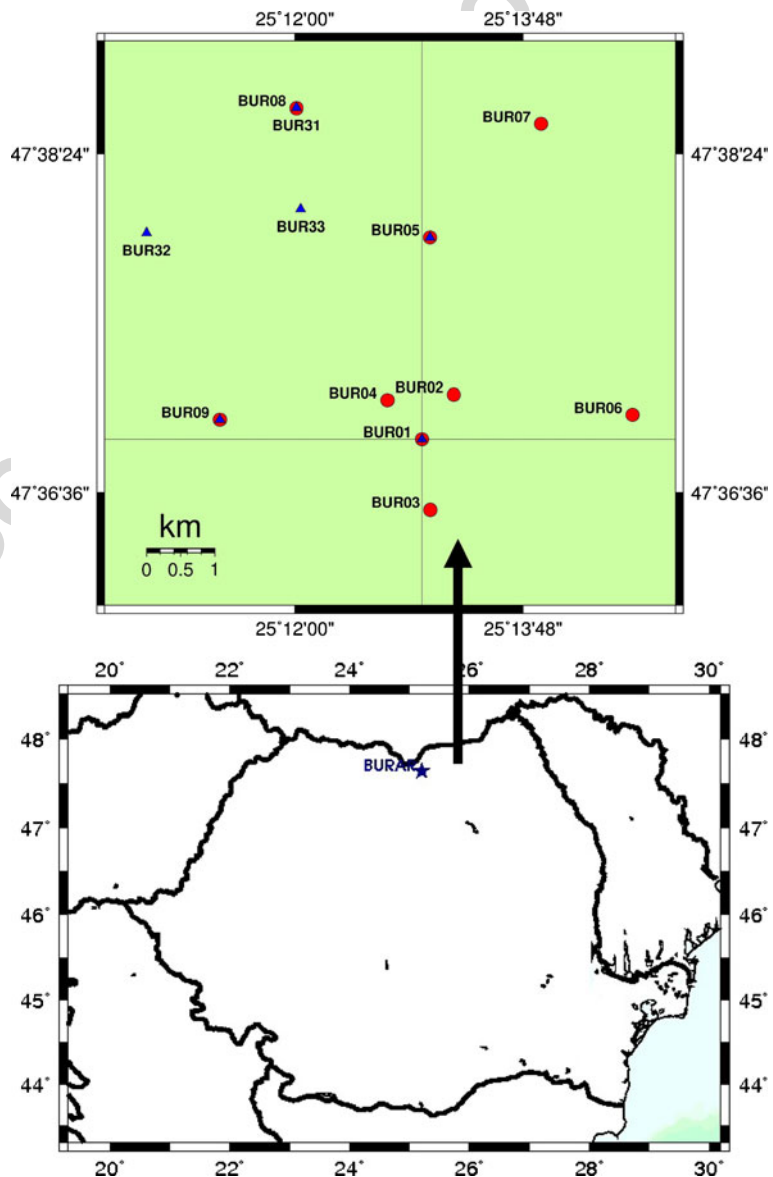
50 of the Ukraine border (Fig. 1). It was installed
 51 in cooperation with the Air Force Technical Ap-
 52 plications Center (USA) and has been operating
 53 since 2002 (Greco et al. 2002).

54 At the beginning, 10 seismic sensors (nine ver-
 55 tical component short-period and one broadband
 56 three-component) were installed in boreholes and
 57 distributed on 5×5 km area. The array was up-
 58 graded in 2008 when five new sensors (CMG40T)
 59 were added: three at the same positions with
 60 BUR01, BUR05, BUR09 and two at new places

(BUR32 and BUR33). All the new sensors have
 three components and are installed at surface.

The short period components have GS-21 seis-
 63 mometers with 1 Hz natural frequency and 0.7
 64 damping constant. AIM24S-1 digitizers provide
 65 24-bit analog to digital converter (ADC) reso-
 66 lution of the seismometer output. The combi-
 67 nation of seismometer gain and digitizer gain
 68 gives a value of 0.0788 nm/s/count at 1 Hz. The
 69 broadband component has a KS54000 sensor with
 70 1 Hz natural frequency and 0.7 damping constant.
 71

Fig. 1 BURAR location on Romania map (*bottom plot*) and array geometry (*top plot*)—*red dots* represent short period sensors and *blue triangles* represent broad band sensors



72 AIM24S-3 digitizers provide 24-bit A-D resolu-
73 tion of the seismometer output. The combina-
74 tion of seismometer gain and digitizer gain gives
75 a value of 0.0404 nm/s/count at 1 Hz. The new
76 CMG40T sensors have 1 Hz natural frequency
77 and 0.7 damping constant and Quantera 330 dig-
78 itizers provide 24-bit analog to digital converter
79 (ADC) resolution of the seismometer output. The
80 combination of seismometer gain and digitizer
81 gain gives a value of 1.192 nm/s/count at 1 Hz
82 We record continuous data with a stream of 40
83 samples per second (sps).

84 The position of the BURAR array is of highest
85 interest since it monitors a large area with poor
86 seismicity, including the East European Platform,
87 the Black Sea shield, Ukraine and the northern
88 part of Romania. It is of equal interest to detect
89 and locate regional events in South-Eastern Eu-
90 rope, the Caucasus and Central Asia. Therefore,
91 we are very interested to calibrate as much as pos-
92 sible the earthquake location parameters, slow-
93 ness and backazimuth, using the BURAR array.

94 In this study, the f - k and plane wave fit analy-
95 ses are used in order to evaluate the ray pa-
96 rameter and backazimuth values as recorded by
97 the BURAR array. Likewise, the Velocity Spec-
98 trum Analysis (VESPA) (Davies et al. 1971) tech-
99 nique is applied to investigate the scattering of
100 P waves. The frequency-wave number analysis
101 (f - k analysis) is able to measure the complete
102 slowness vector (i.e., backazimuth and horizontal
103 slowness) simultaneously. The f - k analysis calcu-
104 lates the power distributed among different slow-
105 nesses and directions of incidence (Capon 1973;
106 Harjes and Henger 1973; Aki and Richards 1980)
107 in the frequency domain. Plane wave fit analy-
108 sis (e.g., Schweitzer et al. 2002) also measures
109 slowness vector and backazimuth but in the time
110 domain.

111 If a plane wave arrives at an array, the signal is
112 recorded at the array stations with a certain time
113 offset depending on the slowness vector of the
114 wave and the position of the station in the array.
115 These time delays are used to specify the slowness
116 or backazimuth of the wave front. The VESPA
117 estimates the seismic energy arriving at the ar-
118 ray for a given backazimuth and different hori-
119 zontal slowness values. Alternatively, the VESPA
120 process can be used for a fixed slowness and

121 varying backazimuths. The result of the VESPA
122 process is displayed as a VESPA gram, a diagram
123 of the seismic energy content (amplitudes) of the
124 incoming signals as a function of slowness or back-
125 azimuth and time.

126 The parameters determined using BURAR
127 records are compared with the theoretical values
128 predicted by the source and station geometry and
129 standard Earth models. Finally, the emphasized
130 deviations are correlated with the tectonic fea-
131 tures and lateral heterogeneities as observed in
132 the Balkan region from the previous studies.

133 The BURAR array is located in the East-
134 ern Carpathian Mountains at an altitude of over
135 1000 m, in a complex tectonic setting character-
136 ized by continental collision at the contact zone
137 between the East European Craton and Carpathi-
138 ans orogen area (Fig. 2).

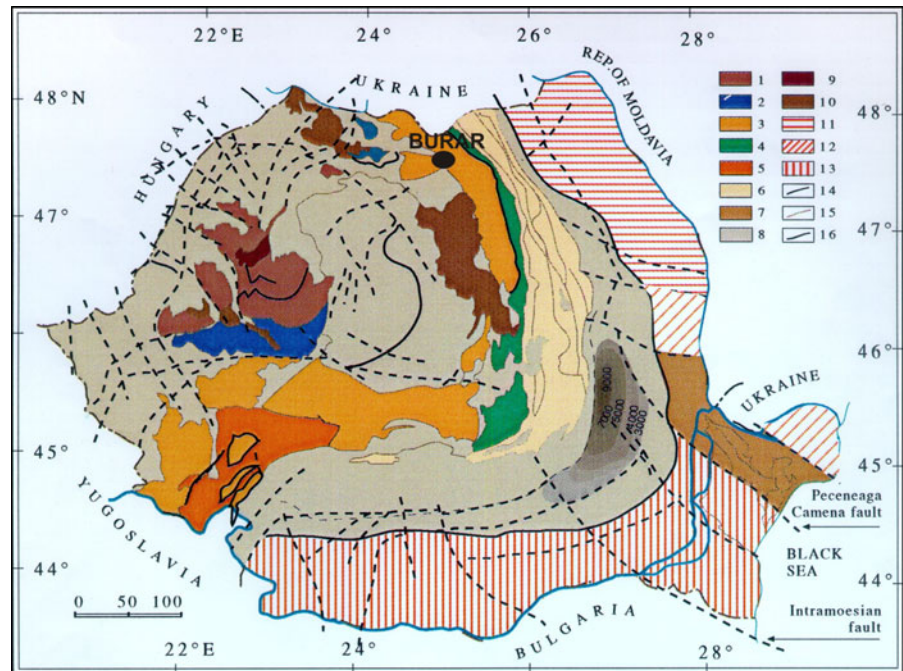
139 The Carpathians fold belt represents a segment
140 of the Tethyan Chain placed and deformed during
141 the Mesozoic and Cenozoic periods (Sandulescu
142 and Visarion 2000) and consists of tectonic units
143 emerging from the deformed lithosphere belong-
144 ing to both the Tethys Ocean (the Main Tethyan
145 Suture) and its continental margins (Southern and
146 Eastern Carpathians).

147 In the Carpathians domain three types of crust
148 can be distinguished:

- 149 – The underthrust forelandic crust type is
150 situated below the cover nappes of the
151 Carpathian Flysch and belongs to the Moesian
152 and Scythian Platforms. Its thickness is vari-
153 able, having the largest values of 45–50 km in
154 the Carpathian Arc Bend Zone.
- 155 – The second crust type is located in Transylva-
156 nia, placed between the Main Tethyan Suture
157 Zone and the “satellite” suture, being char-
158 acterized by a thickness of 26–28 km. Here,
159 the basaltic layer is normally developed, while
160 the granite layer becomes thicker under the
161 central part of the Transylvanian Basin.
- 162 – The third type is the Pannonian crust, which
163 has a thickness of 24–26 km, including a thin
164 basaltic layer (Stanica et al. 2000).

165 The lateral inhomogeneous structure charac-
166 terizes also the entire Alpine-Mediterranean area,
167 which is a wide and complex geophysical system

Fig. 2 Tectonic map of Romania (after Mandrescu and Radulian 1998) with location of the BURAR array—black dot



168 at the confluence of the African, Arabian and
 169 Eurasian blocks. A large amount of research has
 170 been focused on explaining and modelling the P
 171 and S wave velocity structure of the mantle in the
 172 area, ranging from regional to local scales by using
 173 different methods and data. On a regional scale,
 174 velocity structure has been studied for example
 175 by Romanowicz (1980), Spakman et al. (1993)
 176 and Bijwaard et al. (1998). Body wave and sur-
 177 face wave inversions were applied to determine
 178 the lithosphere–mantle structure by Panza et al.
 179 (1980), Calcagnile and Panza (1990), Zielhuis and
 180 Nolet (1994), Marquering and Snieder (1996).

181 **2 Data processing: regional and teleseismic events**

182 For this study we selected a number of 180 re-
 183 gional and teleseismic events with epicentral dis-
 184 tance up to 50° . We considered regional events
 185 if the distance between station and source is in
 186 range of 7° up to 25° and teleseismic events if
 187 the epicentral distance is greater than 25° . The
 188 earthquakes are recorded between 2004 and 2008.
 189 The distribution of the earthquakes shows strong
 190 inhomogeneous azimuth coverage (Fig. 3). Since
 191 the majority of the earthquakes occurred in the

southern part relative to BURAR, the corrections
 of these parameters will be better constrained
 for these regions. The seismic activity is strongly
 inhomogeneous in the study area; therefore, we
 cannot equally cover the entire azimuth domain.

In the case of regional and teleseismic events,
 the backazimuth and ray parameter values were
 determined for P waves using both plane wave
 fit and f - k techniques for a number of 180
 earthquakes. The selected events were divided in
 earthquakes with high and medium SNR and the
 analysis was carried out separately. For the events
 with high SNR (60 events), we calculated these
 parameters for the S waves too. We used wave-
 forms recorded just by the short period BURAR
 elements. The time windows in case of f - k analysis
 were manually selected with lengths between 2
 and 5 s. The picks for the plane wave fit method
 are set manually as well. Note that the station
 heights differences were taken into account when
 applying the both analyses.

For the theoretical calculations, we adopted
 the standard 1-D IASP91 model (Kennett
 1991) and for the parameters of the reference
 earthquakes the data provided by European
 Mediterranean Seismological Center ([http://www.
 emsc-csem.org](http://www.emsc-csem.org)).

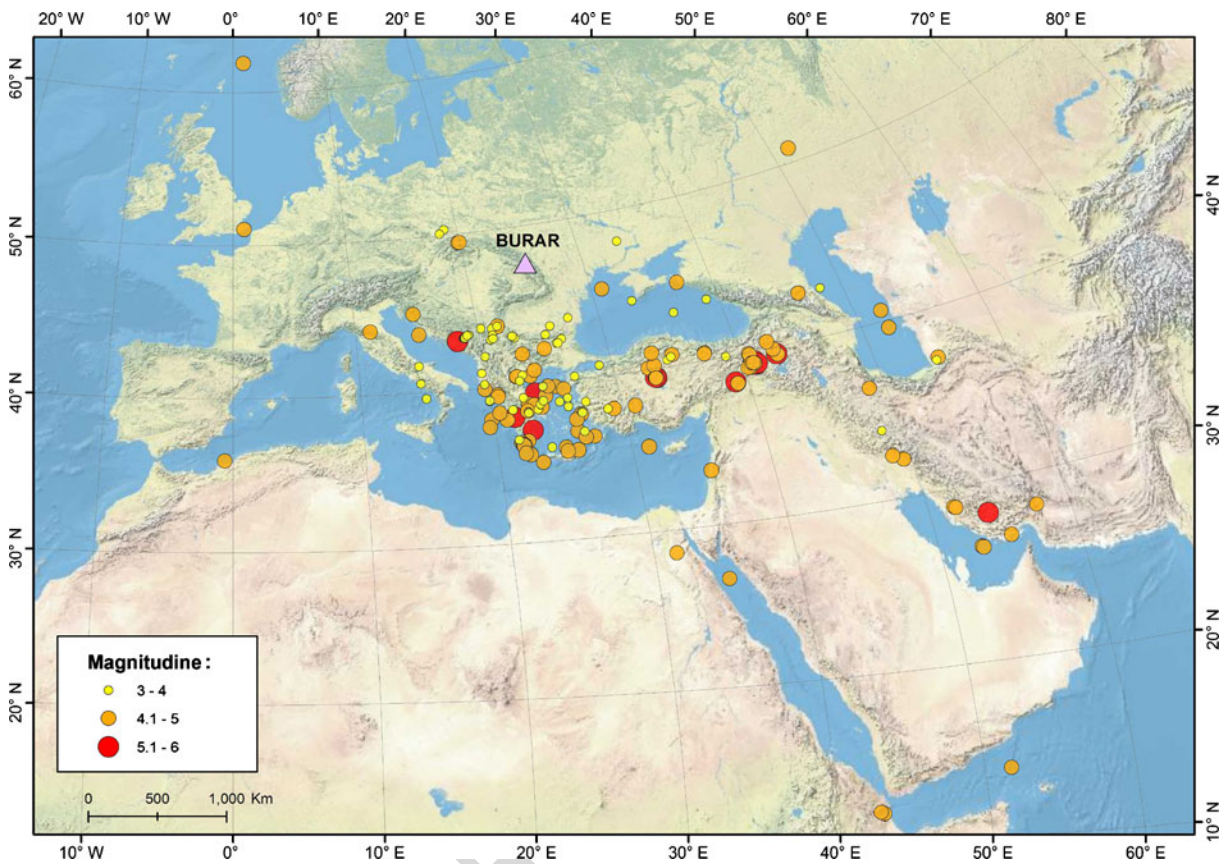


Fig. 3 The distribution of the regional earthquakes (*dots*); *triangle* shows the location of the BURAR array

219 To check for possible local structure differences
 220 beneath stations, we investigate the travel-times
 221 residuals at single stations for the events with best
 222 signal-to-noise ratio and did not find any system-
 223 atic delays.

224 For the *f-k* analysis (Fig. 4) of P waves, we dis-
 225 tinguish two azimuthal segments with major devi-
 226 ations: one is situated between 70° and 150° where
 227 negative backazimuthal deviations are prevalent
 228 signifying deviations of the seismic rays towards
 229 east as compared with the theoretical ray paths;
 230 the other is situated between 160° and 200°, where
 231 positive backazimuthal deviations are prevalent,
 232 showing deviations to the west of the seismic rays.
 233 No systematic deviations are noticed in the in-
 234 terval 200–260° due to the diminishing detection
 235 capacity or poor seismicity.

236 The plane wave fit analysis applied for the same
 237 events (P waves) shows practically a similar dis-
 238 tribution of the backazimuthal deviations (Fig. 4)

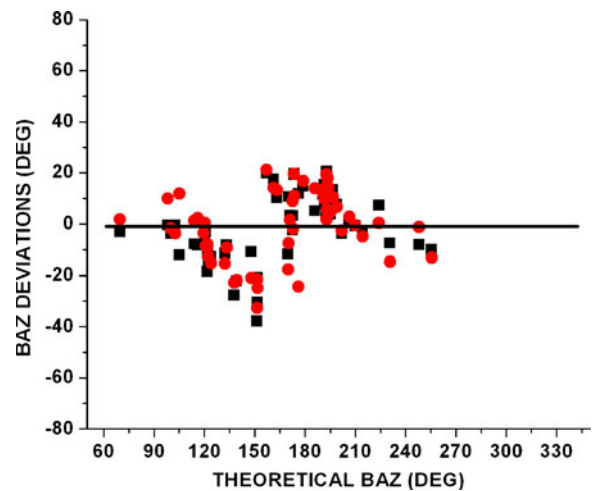


Fig. 4 Backazimuthal deviations resulted from *f-k* (with *black squares*) analysis and plane wave fit analysis (with *red dots*) in the case of P waves for the events with high SNR

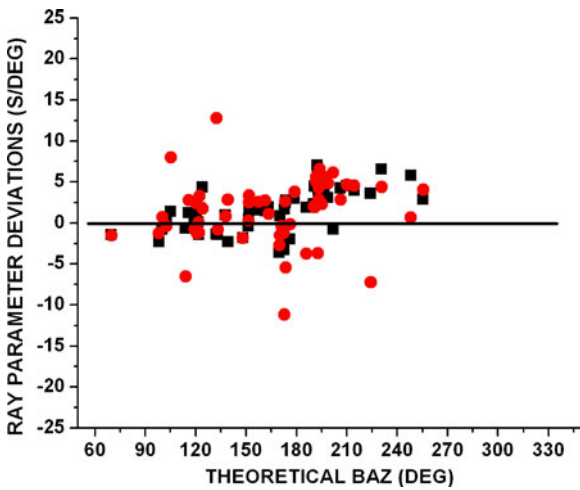


Fig. 5 The ray parameter deviations resulted from f-k (with *black squares*) analysis and plane wave fit analysis (with *red dots*) in the case of P waves for the events with high SNR

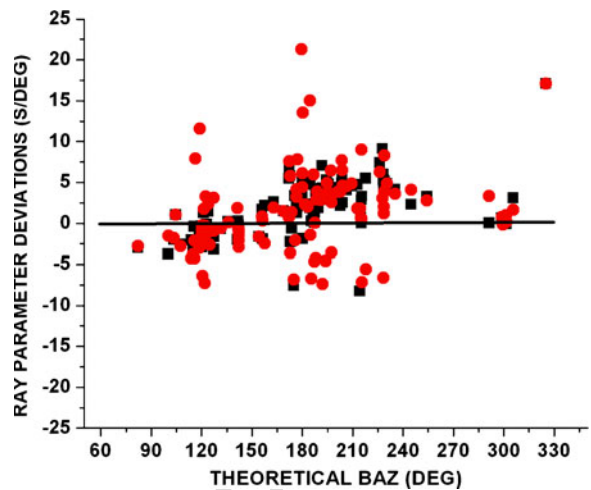


Fig. 7 The ray parameter deviations resulted from f-k (with *black squares*) analysis and plane wave fit analysis (with *red dots*) in the case of P waves for the events with medium SNR

239 with generally smaller deviation values than those
 240 resulted from the f-k analysis (Fig. 5).

241 The investigation of the ray parameter devia-
 242 tions shows values around zero up to 180° and
 243 slightly tendency for positive values from 180° to
 244 260°. Figures 6 and 7 show the results of the f-
 245 k and plane wave fit analysis when considering
 246 the events with medium SNR; in fact, these are

247 represented by events for which P waves entries
 248 are not characterized by impulsivity. The same
 249 patterns are obtained as for the high SNR events,
 250 characterized by a clear impulsive P phase. An
 251 azimuth interval with no earthquakes detected
 252 previously (280° to 320°) has this time a few earth-
 253 quakes recorded. This time the azimuth devia-
 254 tions are higher in case of plane wave fit analysis.

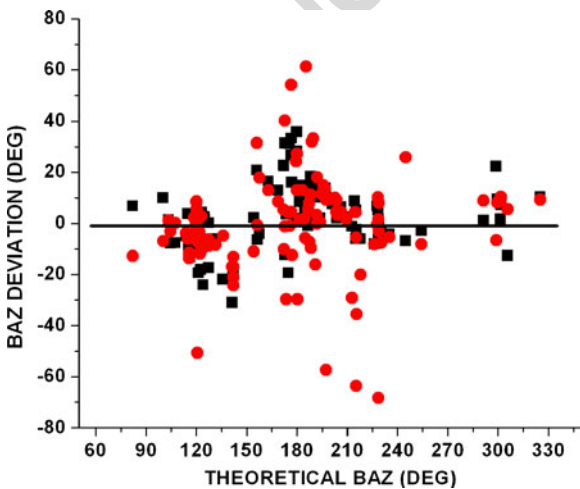


Fig. 6 Backazimuth deviations resulted from f-k (with *black squares*) analysis and plane wave fit analysis (with *red dots*) in the case of P waves for the events with medium SNR

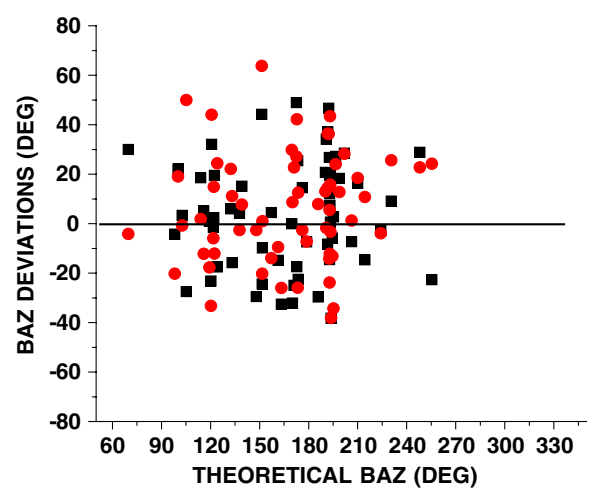


Fig. 8 Backazimuth deviations resulted from f-k (with *black squares*) analysis and plane wave fit analysis (with *red dots*) in the case of S waves for the events with high SNR

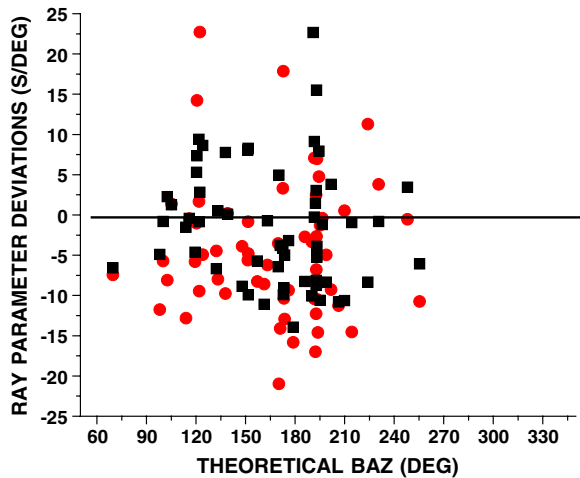


Fig. 9 The ray parameter deviations resulted from f-k (with black squares) analysis and plane wave fit analysis (with red dots) in the case of S waves for the events with high SNR

255 Our investigation shows that the plane wave fit
 256 analysis is very sensitive to the SNR and is not
 257 appropriate to constrain the deviations provided
 258 by the moderate earthquakes. Different filtering
 259 ranges were tested in order to increase signal to
 260 noise ratio. For all events, a Butterworth band
 261 pass filter between 0.8 and 3 Hz can be adopted
 262 as most appropriate for both techniques. Note that

with increasing the frequency range in case of But- 263
 terworth bandpass filter, the onsets were distorted 264
 and became unclear what makes the power of the 265
 signal to be lower. The filtering application leads 266
 to an increase of the signal to noise ratio with an 267
 order of 3. 268

We applied both techniques for S waves in the 269
 case of events with high SNR. It is quite difficult 270
 to appreciate arrivals of different phases (e.g., 271
 S_g, S_n) and the corresponding errors are higher 272
 than in the case of P waves. The distributions 273
 of backazimuth and ray parameter deviations are 274
 more scattered than in case of P waves for events 275
 with high SNR. Both deviations are better defined 276
 using f-k analysis than plane wave fit technique 277
 (Figs. 8 and 9) because the last one requires accurate 278
 identification of arrivals. For S waves, it is 279
 difficult to identify any tendency in backazimuth 280
 and ray parameter deviations. 281

The VESPA diagrams provide a way to identify 282
 the direction of waveforms propagation and 283
 the scattering suffered by the P waves and can 284
 be used to sustain our statements concerning the 285
 backazimuthal deviations for P waves. The time 286
 length used for the VESPA plots was up to 40 s 287
 which contains a small time window before the 288
 first onset and the rest of the plotted seismic 289
 signal. The waveforms have been filtered with 290

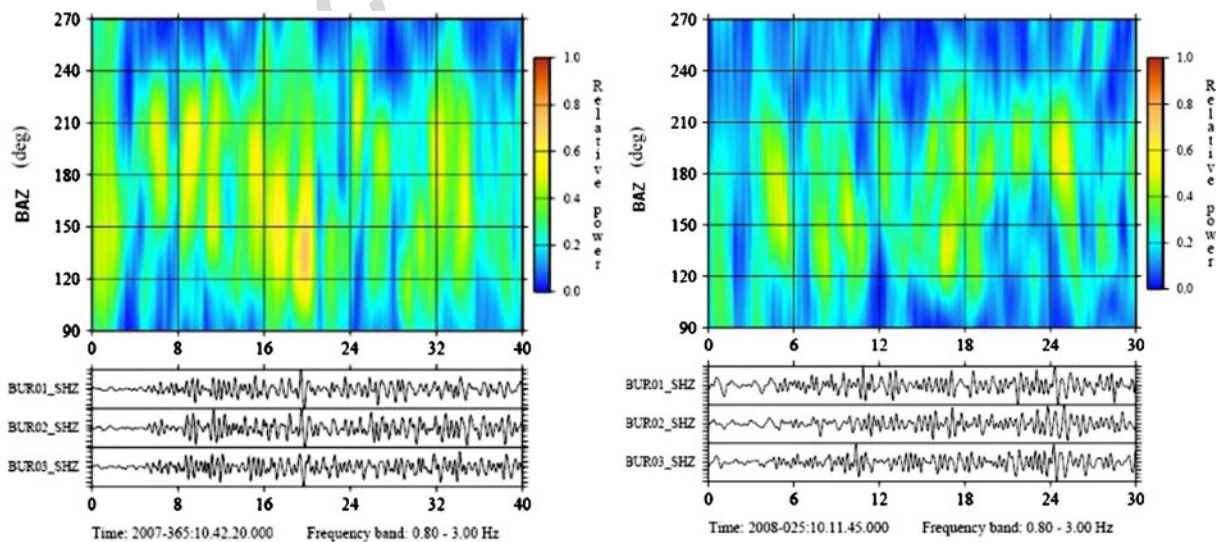
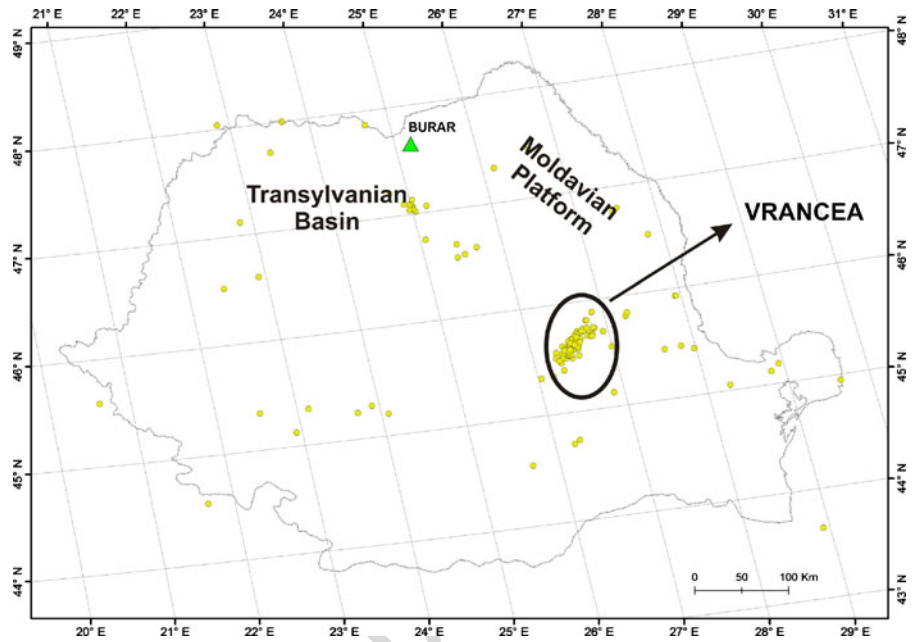


Fig. 10 An example of VESPA gram for the earthquake occurred in the Aegean Sea on 12/31/2007 (left side) and an example of VESPA gram for the earthquake occurred

in Bulgaria on 01/25/2008 (right side). Distinguished outset phases can be associated in the seismogram as regions with high incoming energy

Fig. 11 The distribution of the local earthquakes (dots); triangle shows the location of the BURAR array



291 a Butterworth band pass filter between 0.8 and
 292 3 Hz. Two examples are given in Figs. 10 and
 293 11 for an earthquake in the Aegean Sea ($M_w =$
 294 4.0) and another one which occurred in Bulgaria
 295 ($M_L = 4.0$). In both cases the backazimuth identified in the VESPA gram (203.39° for the first
 296 event and 204.29° for the second one) differ by
 297 about 30° from the theoretical values (171.71° in
 298 the first case and 172.91° in the second case). The
 299 deviations (around 32°) are of the same order as
 300 the deviations obtained by f-k and plane wave fit
 301 analyses.
 302

303 **3 Data processing: local events**

304 The local events are distributed within a radius of
 305 about 4.5° around BURAR. We selected a num-
 306 ber of 121 events with sufficient SNR (>5) for the
 307 BURAR recordings. We treated separately the
 308 shallow earthquakes (52 events with depths be-
 309 tween 0 and 38 km) and intermediate-depth earth-
 310 quakes (69 events with depths situated between
 311 69 and 160 km). We used waveforms recorded
 312 just by the short period BURAR elements. All
 313 the intermediate-depth events are coming from
 314 the Vrancea seismic source, located beneath the
 315 South-Eastern Carpathians Arc bend, at about

350 km epicentral distance from the BURAR 316
 array (Fig. 11). Because the SNR has generally 317
 medium values, we used only f-k analysis and only 318
 P waves. 319

The backazimuth anomalies (Fig. 12) are of the 320
 same order as for the regional events, but this 321
 time we cannot identify segments with systematic 322
 deviations. The ray parameter anomalies (Fig. 13) 323
 are generally small (below 7 s/deg) so that we 324
 conclude that for the crust at local scale the in- 325

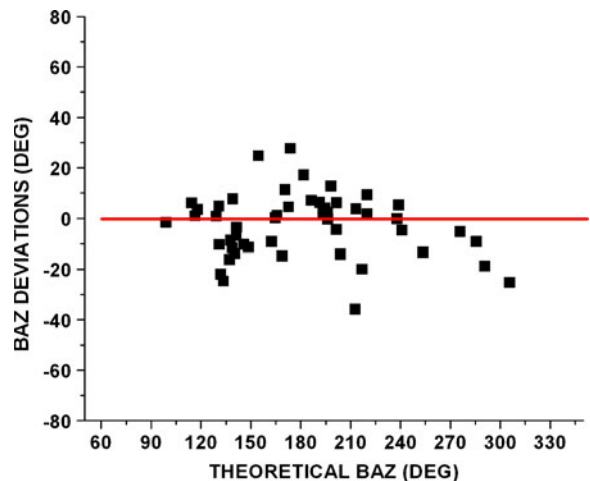


Fig. 12 Backazimuth deviations for the shallow events

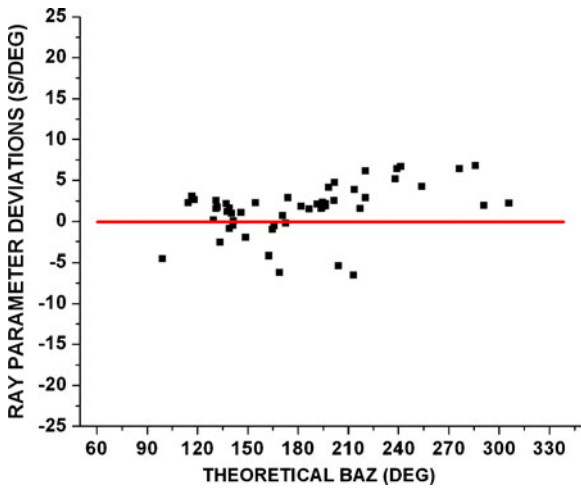


Fig. 13 Ray parameter deviations for the shallow events

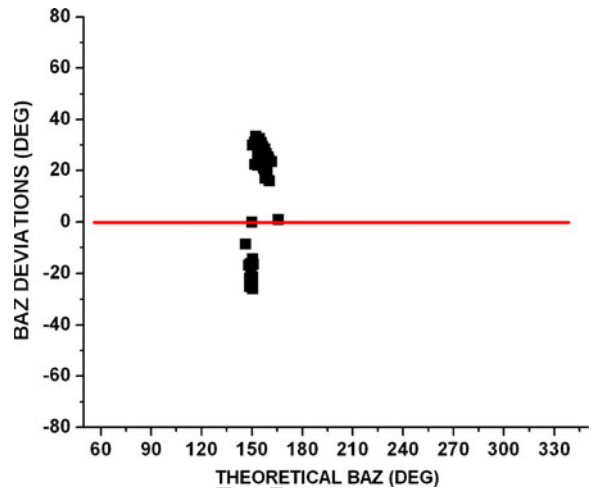


Fig. 15 Backazimuth deviations for the intermediate-depth events

326 homogeneities are not so strong as for the entire
327 lithosphere as revealed at regional scale.

328 At the same time, the VESPA grams outline
329 backazimuthal deviations smaller than in the case
330 of regional events. Two examples are given in the
331 Fig. 14 where the theoretical values of backaz-
332 imuths are 165.12° for the first event (left side)
333 and 186.65° for the second one (right side), while
334 we found from the diagram the values of 164.91°
335 in the first case and 193.66° in the second one.

The intermediate-depth events represent a particular case considering their extreme concentration in space, and also the important backazimuthal deviations (Fig. 15) clustered in two separated groups. The group with negative anomalies is traveling to BURAR through the Moldavian Platform, while the group with positive anomalies is traveling to BURAR through the Transylvanian Basin. Apparently, the azimuth

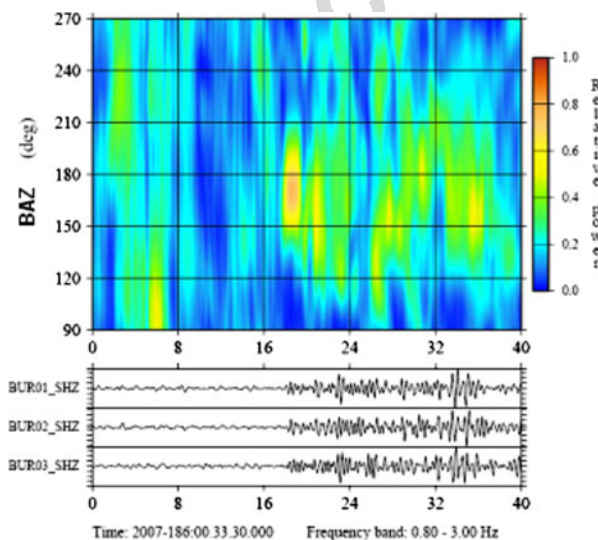
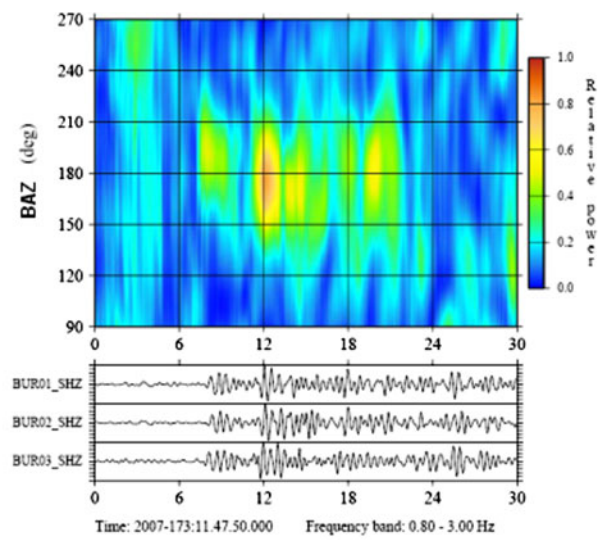


Fig. 14 An example of VESPA gram for the earthquake occurred in Muntenia region (southeastern part of Romania) on 07/05/2007 (left side) and another for the earth-



quake occurred in Transylvania region (western part of Romania) on 06/22/2007 (right side)

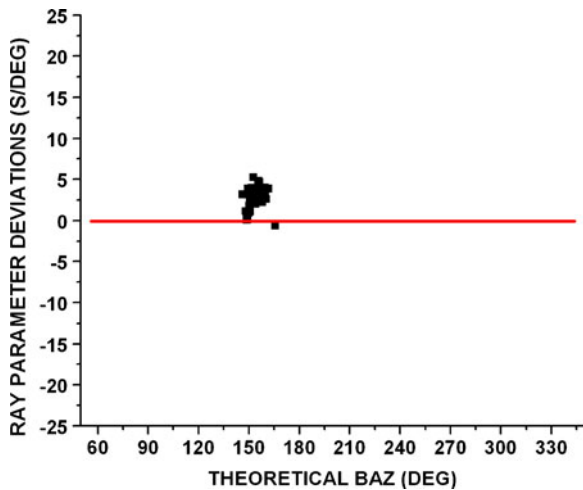


Fig. 16 Ray parameter deviations revealed in case of the intermediate-depth events

345 deviations correlate with the epicentral position
 346 (Fig. 17): negative anomalies for the earthquakes
 347 produced in the northeastern part of the Vrancea
 348 area and positive anomalies for the earthquakes
 349 produced in the southwestern part of the Vrancea
 350 area.

351 The ray parameter deviations are positive but
 352 significantly smaller (Fig. 16) and can be hypothet-
 353 ically explained by the structural heterogeneities
 354 below the array (Fig. 17).

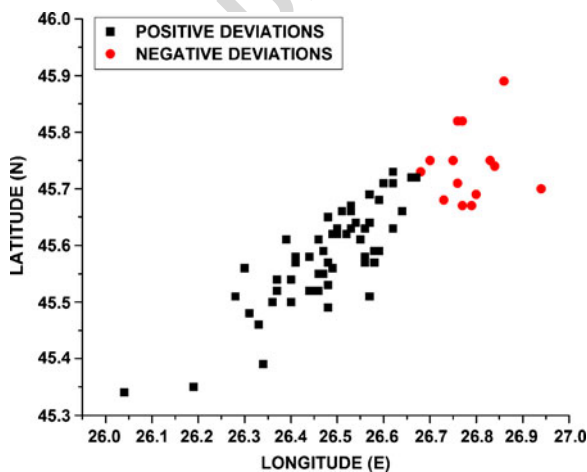


Fig. 17 Distribution of the epicenters of Vrancea earthquakes with the associated backazimuth deviations

4 Conclusions

355

The present paper describes a quality analysis 356
 performed on data recorded by the Bucovina Ar- 357
 ray (BURAR), situated in the northern Romania. 358
 The application of plane-wave fit and f-k tech- 359
 niques to local, regional and teleseismic events 360
 outlines significant anomalies in backazimuth and 361
 ray parameter measurement as compared with the 362
 values predicted by standard IASP91 1-D model. 363
 VESPA-grams of a few selected events confirm 364
 these results. 365

High backazimuth deviations are found for 366
 seismic events from the southern sector, chang- 367
 ing abruptly from negative to positive values be- 368
 tween 150° and 160°. They are more pronounced 369
 in the case of regional and teleseismic events 370
 than local events. Since these deviations create 371
 severe problems regarding the detection capabil- 372
 ities of the BURAR array for the events from 373
 the southern sector, they should be considered as 374
 corrections when using BURAR array in location 375
 procedures. 376

The purpose of this study limits itself to 377
 define the deviations relative to a standard 1-D 378
 model (IASPEI91) using available recordings and 379
 different techniques of investigation and corre- 380
 lated them only qualitatively with the seismotec- 381
 tonic settings of the region. Certainly, a major 382
 step forward in the future work will be to explain 383
 these important anomalies by a local/regional 3-D 384
 model. 385

The bending of the rays coming in the segment 386
 100–140° shows a lateral increase of the velocity 387
 to the east (East European Platform), while the 388
 bending in an opposite direction for the rays com- 389
 ing in the segment 150–200° shows a lateral in- 390
 crease of the velocity to the west. We assume that 391
 the bending effects are larger in the mantle than 392
 in the lithosphere because they are prominent in 393
 the case of regional events. 394

As concerns the ray parameter deviations, they 395
 are not as evident as the backazimuth deviations. 396
 The ray parameter anomalies for regional and 397
 local events may be not significant, as (1) the inci- 398
 dence angle for P_n does not change with distance 399
 and (2) the comparison with IASPEI91 may be 400
 too much simplified, considering the complex ge- 401
 ological situation of the study area. For example, 402

403 the encounter of high-velocity material descend-
404 ing in the asthenosphere beneath the Vrancea
405 region could induce negative anomalies of the
406 ray parameter for the rays passing through this
407 zone.

408 It is well known that in many cases, the ob-
409 served direction deviations are caused by local
410 structure directly beneath the stations. Our tests
411 for BURAR using single station travel time de-
412 lays for the events with high signal-to-noise ratio
413 do not indicate systematic delays, so that, to a
414 first approximation, we can assume that lateral
415 differences in the local structure beneath the array
416 do not significantly influence our interpretation.

417 The main conclusion of our investigation is the
418 observation of considerable anomalies when using
419 BURAR array data for regional and teleseismic
420 events situated in the southern domain as com-
421 pared with standard IASPEI91 model. Clearly,
422 they show significant heterogeneities in the man-
423 tle along this sector and require insertion of ar-
424 ray corrections for location procedures. At the
425 same time, the raw measurements of azimuth and
426 ray parameter as input for corrections contain
427 considerable scatter. Therefore, future efforts are
428 recommended to remove outliers and to define
429 smoothed functions over azimuth and ray para-
430 meter for correction procedures (either as table
431 or fitted analytic function). Alternatively, a list of
432 selected, representative events can be considered,
433 where the closest match can be transferred to
434 the new event. The increase of available database
435 for BURAR and the improving of interpretation
436 by considering regional 3-D modeling are cru-
437 cial steps to implement the results of the present
438 work.

439 **Acknowledgements** This study was performed during a
440 visit to NORSAR under the NERIES program (EC project
441 026130/2006). We are grateful to the Selection Committee
442 of NERIES for that grant. These results are based on
443 the data recorded by BURAR array installed and main-
444 tained in the framework of the bilateral cooperation be-
445 tween the Air Force Technical Application Center (USA)
446 and the National Institute for Earth Physics (Romania).
447 We are grateful to the editor Frank Krueger and to the
448 two reviewers whom suggestions and critical remarks con-
449 tributed to improve significantly the quality of the paper
450 presentation.

References

- 451
- Aki K, Richards PG (1980) Quantitative seismology, vol. I
and II. Freeman, San Francisco, pp 932 452
453
- Bijwaard H, Spakman W, Engdahl ER (1998) Closing the
gap between regional and global travel time tomogra-
phy. *J Geophys Res* 103:30055–30078 454
455
- Calcagnile G, Panza GF (1990) Crust and upper mantle
structure of the Mediterranean area derived from sur-
face wave data. *Phys Earth Planet Inter* 60:163–168 456
457
- Capon J (1973) Signal processing and frequency wavenum-
ber spectrum analysis for a large aperture seismic
array. In: Bolt B (ed) *Methods in Computational*
Physics, vol 13. Academic, New York, pp 473 458
459
- Davies D, Kelly EJ, Filson JR (1971) The VESPA process
for the analysis of seismic signals. *Nature* 232:8–13 460
461
- Greu B, Ghica D, Popa M, Rizescu M, Ionescu C (2002)
Earthquake monitoring by the seismic network of the
National Institute for Earth Physics. *Rev Roum Geo-*
phys 46:47–57, Bucuresti 462
463
- Harjes H-P, Henger M (1973) Array-seismologie. *Z Geo-*
phys 39:865–905 (in German) 464
465
- Kennett BLN (ed) (1991) IASPEI 1991 Seismological Ta-
bles. Research School of Earth Sciences, Australian
National University, pp 167 466
467
- Mandrescu N, Radulian M (1998) Characterization of seis-
mogenic zones of Romania, EEC Tehnical Report,
Project CIPA-CT94-0238 468
469
- Marquering H, Snieder R (1996) Surface-wave velocity
structure beneath Europe, the northeastern Atlantic
and weastern Asia from waveform inversion including
surface-wave mode coupling. *Geophys J Int* 127:283–
304 470
471
- Panza GF, Calcagnile G, Scandone P, Mueller S (1980)
Struttura profonda dell'area mediterranea. *Le Scienze*
24:60–69 472
473
- Romanowicz BA (1980) A study of large-scale lateral vari-
ations of P velocity in the upper mantle beneath West-
ern Europe. *Geophys J R Astr Soc* 6(1):217–232 474
475
- Rost S, Thomas C (2002) Array seismology: methods and
applications. *Rev Geophys* 40(3):1008. doi:10.1029/
2000RG000100 476
477
- Sandulescu M, Visariom M (2000) Crustal structure and
evolution of Carpathian-western Black Sea areas. *First*
Break 18:103–108 478
479
- Schweitzer J, Fyen S, Mykkeltveit, T Kvérna (2002)
IASPEI – New manual of seismological Observatory
practice, tom 1, Chapter 9, Potsdam 480
481
- Spakman W, van der Lee S, van der Hilst RD (1993)
Travel-time tomography of the European- Mediter-
ranean mantle down to 1400 km. *Phys Earth Planet*
Inter 79:3–74 482
483
- Stanica D, Stanica M, Asimpolos L (2000) The main
Tethyan suture zone revealed by magnetotelluric to-
mography. *Rev Roum Geophys* 44:123–130, Bucuresti 484
485
- Wessel P, Smith WHF (1995) New version of the generic
mapping tools released. *Eos Trans* 76:329 486
487
- Zielhuis A, Nolet G (1994) Shear-wave velocity variations
in the upper mantle beneath central Europe. *Geophys*
J Int 117:695–715 488
489

AUTHOR QUERIES

AUTHOR PLEASE ANSWER ALL QUERIES

- Q1. Figure 5 citation was inserted here. Please check if appropriate.
- Q2. Quality of Figures 10 and 14 are below publishing standard. Please provide better quality figures. Otherwise, please confirm if okay to proceed with the originally processed figures.
- Q3. Figure 17 citation was inserted here to arrange figure citations in sequential order.
- Q4. References (Rost and Thomas 2002; Wessel and Smith 1995) were not cited in text. Please provide corresponding citation.

UNCORRECTED PROOF